Recurrence networks to study dynamical transitions in a turbulent combustor

V. Godavarthi, V. R. Unni, E. A. Gopalakrishnan, and R. I. Sujith

---

Articles you may be interested in

Recurrence networks to study dynamical transitions in a turbulent combustor

V. Godavarthi,[1] V. R. Unni,[1] E. A. Gopalakrishnan,[2,a)] and R. I. Sujith[1]

[1]*Department of Aerospace Engineering, IIT Madras, Chennai 600036, India*
[2]*Center for Computational Engineering and Networking, Amrita School of Engineering,*
Amrita Vishwa Vidyapeetham (Amrita University), Coimbatore 641112, India

Thermoacoustic instability and lean blowout are the major challenges faced when a gas turbine combustor is operated under fuel lean conditions. The dynamics of thermoacoustic system is the result of complex nonlinear interactions between the subsystems—turbulent reactive flow and the acoustic field of the combustor. In order to study the transitions between the dynamical regimes in such a complex system, the time series corresponding to one of the dynamic variables is transformed to an ε-recurrence network. The topology of the recurrence network resembles the structure of the attractor representing the dynamics of the system. The transitions in the thermoacoustic system are then captured as the variation in the topological characteristics of the network. We show the presence of power law degree distribution in the recurrence networks constructed from time series acquired during the occurrence of combustion noise and during the low amplitude aperiodic oscillations prior to lean blowout. We also show the absence of power law degree distribution in the recurrence networks constructed from time series acquired during the occurrence of thermoacoustic instability and during the occurrence of intermittency. We demonstrate that the measures derived from recurrence network can be used as tools to capture the transitions in the turbulent combustor and also as early warning measures for predicting impending thermoacoustic instability and blowout. *Published by AIP Publishing.* [http://dx.doi.org/10.1063/1.4985275]

Combustors operating under fuel lean conditions are highly susceptible to thermoacoustic instability and lean blowout. When there is a positive feedback between the unsteady heat release rate and the acoustic field in a combustor, high amplitude acoustic oscillations occur. This condition is referred to as thermoacoustic instability. These high amplitude acoustic oscillations result in the enhancement of heat transfer to the walls and structural damage to the engine. As the equivalence ratio of combustion is reduced below a critical value, the flame inside the combustor ceases to exist, resulting in the situation referred to as flame blowout. In the past few decades, studies have been conducted to predict thermoacoustic instability and blowout in a turbulent combustor as well as to determine the dynamics underlying the transitions between the dynamical regimes in a combustor. The presence of the nonlinear interactions between the subsystems warrants that the thermoacoustic system is a complex system. These interactions between the subsystems also result in the presence of multiple time scales in a thermoacoustic system during the occurrence of aperiodic oscillations known as combustion noise. In this paper, we transform the time series data of acoustic pressure from a turbulent combustor to an ε-recurrence network. Recurrence network (RN) preserves the geometry of the attractor. The geometry of the attractor is changed when there is a transition between the dynamical regimes. In our present work, we study the variation of the degree distribution with recurrence threshold. We also investigate the variation of network properties with the equivalence ratio in a turbulent combustor. Summing up the results, we show that RN can be used as a tool to capture the transitions between the dynamical regimes in a combustor.

I. INTRODUCTION

Thermoacoustic instability arises when there is positive feedback between the unsteady heat release rate and the acoustic field in a combustor.[1] Thermoacoustic instability results in large amplitude acoustic oscillations, which lead to the enhancement in the heat transfer to the walls and also lead to the structural damage to the engine. The other challenge faced is flame blowout. Blowout occurs when the flame cannot be stabilized and ceases to exist in the combustion chamber, as the equivalence ratio (the ratio of the actual fuel/air ratio to the stoichiometric fuel/air ratio) is reduced below a critical value. In aircrafts, blowout results in the loss of the thrust generated and the flame has to be re-ignited. Blowout might also lead to a sudden drop in the altitude of the aircraft. Various studies have been conducted to predict impending thermoacoustic instability and blowout. Recent studies show that the transitions in a turbulent combustor exhibit rich dynamical behavior.[2] Hence, there is an exigency to investigate and characterize the dynamics underlying the transitions to thermoacoustic instability and blowout in a turbulent combustor.

a)Author to whom correspondence should be addressed: ea_gopalakrishnan@cb.amrita.edu

In many turbulent combustors, the transitions happen from combustion noise to thermoacoustic instability and from thermoacoustic instability to lean blowout when the equivalence ratio is varied from fuel rich to fuel lean conditions. Combustion noise is composed of low amplitude aperiodic pressure oscillations that occur during the stable operation of a combustor. Tony *et al.*[3] showed that combustion noise has the features of a high dimensional chaotic signal contaminated with white and colored noise, using a plethora of tools to ascertain the determinism. Nair *et al.*[4] suggested that the transition from combustion noise to thermoacoustic instability can be considered as a transition from a chaotic state to an ordered state. In their subsequent work, Nair and Sujith[5] reported that combustion noise has a complex scaling behavior and used multifractal spectrum to characterize this. Further, they reported the loss of multifractality in the signal at the onset of thermoacoustic instability. Nair and Sujith[5] demonstrated that Hurst exponent, a measure of the fractal dimension of a time series, can be used as a precursor to predict thermoacoustic instability. Nair *et al.*[6] also illustrated that the transition from combustion noise to thermoacoustic instability happens via intermittency, a state composed of bursts of large amplitude periodic oscillations amidst low amplitude aperiodic oscillations.

After the transition from combustion noise to thermoacoustic instability, on further reduction in the equivalence ratio, the transition happens from thermoacoustic instability to lean blowout. This transition from thermoacoustic instability to lean blowout exhibits a rich dynamical behavior. Kabiraj *et al.*[7,8] detected intermittency prior to blowout in laminar premixed combustion. Gotoda *et al.*[9] studied the transitions from combustion instability to blowout and detected the presence of multifractal characteristics in the reconstructed phase space prior to lean blowout. In a subsequent work, Gotoda *et al.*[10] demonstrated that the various nonlinear quantities such as translational error and permutation entropy can be used as early warning signals to predict blowout. Extending the work of Nair and Sujith,[5] Unni and Sujith[11] provided a multifractal description to the oscillations prior to lean blowout, thus providing a unified framework to study the transition from combustion noise to thermoacoustic instability and then to blowout. They suggested that Hurst exponent can be a precursor to blowout.

The nonlinear interactions between the acoustic field, the hydrodynamic field, and the unsteady combustion resulting in different dynamical regimes varying from combustion noise (chaos) to thermoacoustic instability (order) in a combustor suggest that a thermoacoustic system can be treated as a complex system. In a complex system, the interaction between components is nonlinear such that the collective behavior of the system is different from the sum of their individual behaviors. These components can self-organize and exhibit a coherent behavior.[12] This refers to a phenomenon called emergence in complex systems.[13] We presume that the emergence of thermoacoustic instability (order) from combustion noise (chaos) and the appearance of discrete scales during the occurrence of thermoacoustic instability in contrast to the multiple scales present during the occurrence of combustion noise might be due to self-organization in the

system. The traditional reductionist approach which monitors individual elements is no longer sufficient to describe the emergent behavior of complex systems.[14]

Complex networks are used to study complex systems[15–17] as they help in understanding the connectivity pattern. Complex networks comprise nodes and links. Nodes represent the components of the system and links represent the interactions between these components. The topology and the measures derived from a network can be used to characterize the qualitative and quantitative behavior of a complex system. The variation in the dynamics of a system is reflected in the topology of the network. The measures derived from complex networks can be used to analyze the transitions between the dynamical regimes in a complex system.[18] The underlying dynamics of a physical system is preserved in the time series data. Hence, in order to study complex systems, time series data from such systems are converted into complex networks. Modeling the network structure is crucial to understand the underlying dynamics of the system. Many methods have been devised to convert the time series into complex networks.[19–22] Strozzi *et al.*[23] have shown that time series can be converted into complex networks and vice versa.

Murugesan and Sujith[24] introduced complex networks to analyze the dynamical regimes in the thermoacoustic system. They used a visibility algorithm to convert the time series to complex networks.[25] The visibility algorithm considers a data point of the time series as a node. Two nodes are connected if they satisfy a visibility condition. (The line connecting the two data points should not intersect the height of an intermediate data point.) They detected a scale-free behavior during the occurrence of combustion noise and regularity at the onset of thermoacoustic instability. Further, Murugesan and Sujith[26] showed that the quantities derived from complex networks such as characteristic path length (CPL) (indicates the average of the minimum number of steps required to reach from one node to another), clustering coefficient (a measure that provides the local clustering or cliquishness of a node), network diameter (the maximum distance between two nodes in a network), and global efficiency (how efficiently a node can be reached from the other nodes in the network) can be used as precursors to predict the onset of thermoacoustic instability and blowout.

While converting the time series into a complex network using a visibility algorithm, information related to the geometry and structure of the attractor is lost. In order to preserve the geometric characteristics of the attractor, we use ε–recurrence networks (RN). RN preserves the information related to the geometry of the attractor. Further, as recurrence is a fundamental property of any deterministic dynamical system, the rationale behind constructing complex networks from time series using recurrence networks is more natural and simpler than visibility networks.[27]

RN does not depend on temporal correlations explicitly. Thus, RN is more robust than other methods that consider temporal correlations such as detrended fluctuation analysis,[28] in the cases where there is external noise in the system.[29] Constructing RN from a time series requires lesser number of data points than those required for computing

Lyapunov exponent. Hence, compared to Lyapunov exponent, measures derived from RN are well suited to discriminate between chaotic and periodic states when a shorter time series is available.[29]

In our present work, we construct RN from the time series of acoustic pressure obtained from a turbulent combustor. The recurrence threshold is chosen by the approach proposed by Jacob *et al.*,[30] which determines an admissible range for ε. Hence, the choice of the recurrence threshold is not arbitrary. We demonstrate that RN preserves the geometry of the attractor and hence the topologies of RNs constructed for various dynamical regimes in a turbulent combustor are different. We study the variation of the degree distribution of RN with ε. We proceed to investigate the variation of RN measures with the equivalence ratio in order to analyze the transitions to thermoacoustic instability and blowout. To the best of our knowledge, this is the first application of RN to study the thermoacoustic instability and blowout.

In Sec. II, we describe the methodology to convert time series into ε–recurrence networks. The experimental setup is described in Sec. III. The results are presented in Sec. IV. Finally, the conclusions are described in Sec. V.

II. ANALYSIS OF DYNAMICS USING RECURRENCE NETWORKS

A. From time series to ε–recurrence networks

There are several methods to generate complex networks from a time series; ε–recurrence method is one of them. In this method, we compute the recurrences of phase space vectors after reconstructing the phase space using Takens' embedding theorem.[31] The discretely sampled experimental time series $x(1), x(2),\ldots x(N_T)$ is embedded in an M-dimensional phase space using an appropriate time delay, where N_T is the total number of points in the time series. The delay vectors are given by

$$X(t_i) = x(i), x(i + \tau), \ldots\ldots, x(i + (M - 1)\tau). \quad (1)$$

In this paper, the embedding dimension M is chosen using Cao's algorithm.[32] The first minimum of the average mutual information is chosen to be the time delay for computing delay vectors from the discretely sampled time series.

A state (phase space vector) $X(t_i)$ is said to be recurrent if there are t_i and t_j such that $d(X(t_i), X(t_j)) < \varepsilon$, where $d(X(t_i), X(t_j))$ is the distance between the phase space vectors $X(t_i)$ and $X(t_j)$, computed using the Euclidean norm and ε is the recurrence threshold. The structure of the recurrences in the phase space is encoded in the recurrence matrix,[33,34]

$$R_{i,j} = \theta(\varepsilon - ||X(t_i) - X(t_j)||). \quad (2)$$

Here, θ is the Heaviside function.

We consider only the spatial interdependencies in recurrence networks. To construct a recurrence network from the time series, we use the adjacency matrix $A_{i,j}$ computed using the recurrence matrix $R_{i,j}$ according to the relation[27]

$$A_{i,j} = R_{i,j} - \delta_{i,j}, \quad (3)$$

where $A_{i,j}$ is the adjacency matrix and $\delta_{i,j}$ is the Kronecker delta. $\delta_{i,j} = 1$ when $i = j$ and $\delta_{i,j} = 0$ when $i \neq j$.

The adjacency matrix provides information regarding the nodes and the connections between them. If $A_{i,j} = 1$, then the nodes i, j are connected, which implies that the state space vectors are in a proximity of the recurrence threshold ε in the phase space.

The measures derived from the recurrence matrix characterize the dynamical properties of phase space trajectories in contrast to the measures derived from RN, which describe the geometrical properties of the attractor. A dynamical property characterizes the dynamics of the system, i.e., regular or irregular dynamics, whereas a geometrical property characterizes the geometry and structure of the reconstructed phase space. Recurrence network provides additional measures from the complex network theory to characterize the geometric properties of the attractor. Hence, RN provides more tools for the analysis of time series.[35]

A crucial parameter in constructing the network is the recurrence threshold ε. If the threshold is very large, the network becomes very dense as there are too many links leading to false recurrences. On the other hand, if the recurrence threshold is too small, the network breaks down into mutually disjointed components. Hence, the network characteristics can become ambiguous. After embedding, the size of the attractor depends on the range of the signal. The time series data are transformed into uniform deviate. Thereby, the attractor size is rescaled into the interval [0, 1].

A random time series is generated and the embedding dimension is chosen to be the same as that of the time series of acoustic pressure obtained from the combustor. Recurrence networks are then constructed from the time series data of acoustic pressure and the random time series. The characteristic path length (*CPL*), the average of the shortest paths between two nodes, is computed for the networks constructed from time series data of acoustic pressure and from random time series. The brief description of *CPL* is provided in Sec. II B. The *CPL* of RN constructed from the time series acquired during combustion noise decreases with the increase in the threshold beyond ε_1 (Fig. 1). When the threshold is ε_1, then a cluster of nodes is formed. Thus, a further increase in
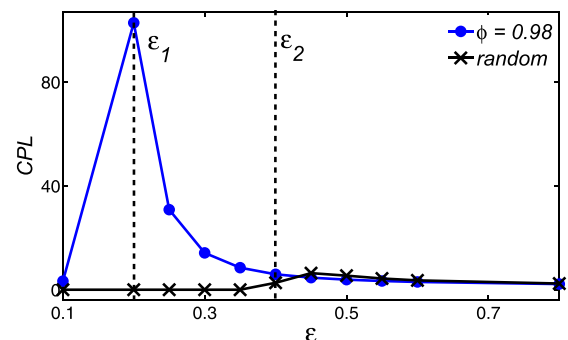

FIG. 1. Variation of the characteristic path length (*CPL*) of recurrence networks with threshold, constructed from both random time series and the time series corresponding to combustion noise. The time series corresponding to combustion noise is embedded in $M = 10$ dimensions and the random time series is also embedded in the same dimension.

threshold results in an effective decrease in *CPL* as the degree of each node increases. When the recurrence threshold is greater than ε_2, the *CPL* of the time series corresponding to combustion noise becomes nearly the same as that of random time series. This is due to the false recurrences. Hence, the upper bound and the lower bound are fixed for the recurrence thresholds as $\varepsilon_1 = 0.2$ and $\varepsilon_2 = 0.4$, respectively. We use $\varepsilon = 0.25$ for our present work. Having an ε above the lower threshold ensures that the network has no disconnected nodes. Having the threshold ε below the upper threshold also ensures that RN constructed from the time series of acoustic pressure is different from the RN constructed from a random time series.

In Subsec. II B, we provide a brief description of the measures derived from RN such as degree distribution, characteristic path length, and betweenness centrality, which are used to analyze the transitions in the thermoacoustic system.

B. Measures describing the topological properties of the network

The following measures are computed from the adjacency matrix A, which encodes the information related to the connectivity of each node.[36]

1. Degree distribution

Degree distribution is the graph plotted between $P(k)$ and k where $P(k)$ is the probability of a given node to have a degree k. $P(k)$ is given by $n(k)/N$ where $n(k)$ is the number of nodes having the degree k and N is the total number of nodes. The degree of a node k_i represents the connectivity of the node. The degree of a node i is the sum of all the elements in the ith row of the adjacency matrix. As the topology of RN resembles the structure of the attractor, the local connectivity of the nodes is related to the local phase space density of the attractor.[36] Thus, the variation in the degree distribution reflects the variation of the local phase space density over the attractor.

2. Betweenness centrality

Betweenness centrality computes the fraction of shortest paths passing through a vertex (node)

$$b_v = \sum_{i,j \neq v}^{N} \frac{\hat{\sigma}_{i,j}(v)}{\hat{\sigma}_{i,j}}, \tag{4}$$

where $\hat{\sigma}_{i,j}$ gives the number of shortest paths between two nodes i and j. $\hat{\sigma}_{i,j}(v)$ gives the number of shortest paths between the nodes i and j that are passing though the node v. The shortest path between the nodes i, j is computed by calculating the minima of all the path lengths between the two nodes i, j in the network represented by the adjacency matrix. Betweenness centrality determines bottleneck nodes or the regions of low phase space density that connect two regions of high phase space density.

3. Characteristic path length

Characteristic path length is the average of the length of the shortest paths between two nodes

$$CPL = \frac{1}{N(N-1)} \sum_{i,j-1}^{N} d_{i,j}, \tag{5}$$

where $d_{i,j}$ is the length of the shortest path between a pair of nodes (i, j), which is nothing but the minimum number of links between node i and node j. We do not consider the disconnected nodes while calculating *CPL*.

III. EXPERIMENTAL SETUP

The schematic of the experimental setup is shown in Fig. 2. The time series of acoustic pressure analyzed in our present work is acquired from a backward facing step combustor with a bluff body used as the flame stabilizing mechanism. The cross section area of combustor is $90 \times 90 \, \text{mm}^2$. The bluff body is a circular disc whose diameter and thickness are 47 mm and 10 mm, respectively. The bluff body is positioned 50 mm from the dump plane inside the combustor. Liquid petroleum gas (LPG) used as the fuel is injected 120 mm upstream of the bluff body. A spark plug positioned at the dump plane is used for ignition. The uncertainty of the mass flow controllers is $\pm (0.8\%$ of reading $+ 0.2\%$ of full scale). The pressure measurements are performed using a PCB106B50 piezoelectric transducer located 90 mm from the backward facing step with an uncertainty of ± 0.15 Pa. The pressure measurements are sampled at a frequency of 10 kHz and the fuel flow rate is 1.04 g/s. The detailed description of the experimental setup is given by Unni and Sujith,[11] and Nair and Sujith.[5]

IV. RESULTS

We observe the transitions from combustion noise to thermoacoustic instability and then to lean blowout as the equivalence ratio (ϕ) is varied. We varied the equivalence ratio (ϕ) from 0.98 to 0.29 in this study. When the equivalence ratio is closer to 1, we observe combustion noise and when we approach the equivalence ratio of 0.29, blowout occurs. The time series of acoustic pressure is plotted for various equivalence ratios in Fig. 3. When the equivalence ratio is 0.98, we observe combustion noise composed of aperiodic fluctuations [Fig. 3(a)]. When the equivalence ratio is 0.8, we observe intermittency [Fig. 3(b)], which consists of large amplitude periodic fluctuations amidst aperiodic oscillations. The equivalence ratio is reduced to 0.77 [Fig. 3(c)], the number of intermittent bursts is increased, and the onset
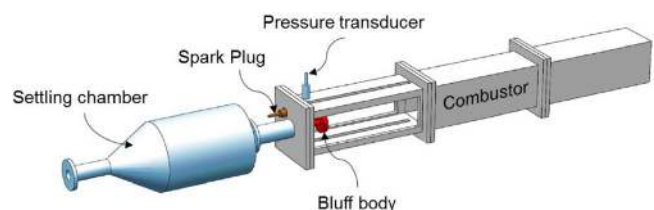
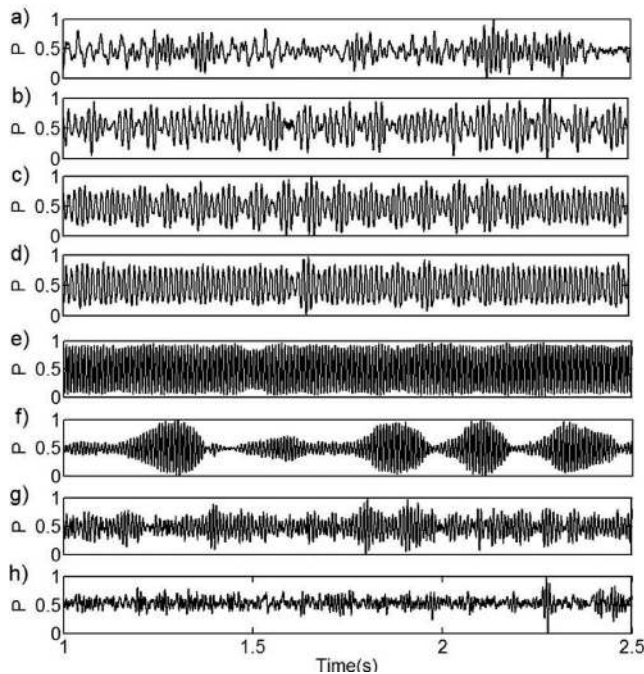

FIG. 2. Schematic of experimental setup.

FIG. 3. The time series of acoustic pressure for various equivalence ratios (a) 0.98, (b) 0.8, (c) 0.77, (d) 0.74, (e) 0.5, (f) 0.47, (g) 0.44, and (h) 0.29, respectively. The amplitude of the acoustic pressure is scaled to the interval [0,1].
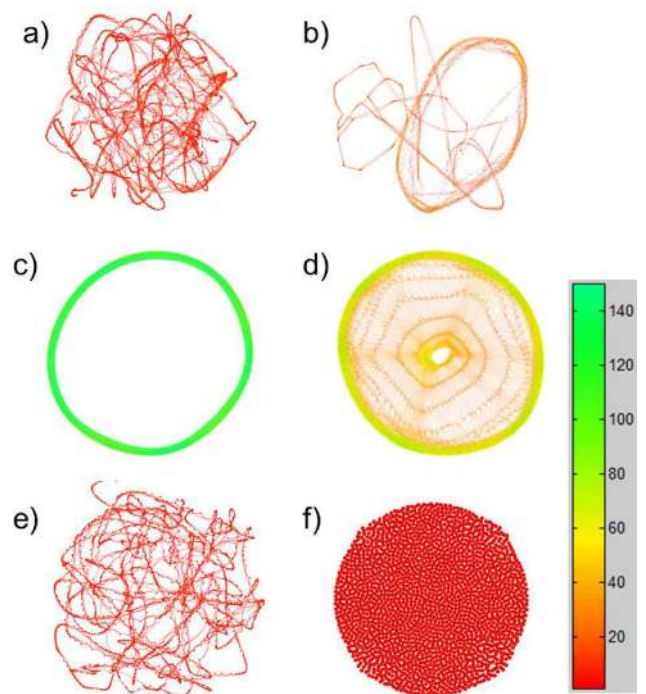

FIG. 4. The topologies of recurrence networks constructed from the time series of acoustic pressure for the equivalence ratios (a) 0.98 (combustion noise), (b) 0.8 (intermittency prior to thermoacoustic instability), (c) 0.5 (thermoacoustic instability), (d) 0.47 (intermittency just after thermoacoustic instability), (e) 0.29 (oscillations prior to lean blowout), and (f) white noise. The networks are constructed from 2000 data points and the recurrence threshold is 0.25. The colorbar shows the variation of the color with the degree of the nodes. This figure reaffirms that RN preserves the geometry of the attractor.

of periodic oscillations can be seen when the equivalence ratio is further reduced to 0.74 [Fig. 3(d)]. As the equivalence ratio is further reduced to 0.5, we observe thermoacoustic instability [Fig. 3(e)]. On further reduction of equivalence ratio to 0.47, we observe that intermittency sets in Fig. 3(f). The equivalence ratio is further reduced to 0.44, and the amplitude and the duration of the periodic bursts in intermittency are decreased [Fig. 3(g)]. When the equivalence ratio is reduced to 0.29, we observe low amplitude aperiodic oscillations [Fig. 3(h)]. If we reduce the equivalence ratio further, the flame blows off.

Thus, as we progress from combustion noise to thermoacoustic instability, the periodicity of the signal increases. We also observe that on further reduction of equivalence ratio, during the transition from thermoacoustic instability to lean blowout, the periodicity of the signal decreases. On further reduction in the equivalence ratio, prior to lean blowout the periodicity of the time series signal is lost. This can be seen from the power spectra of time series (FFT). The power spectra of the same pressure time series are plotted by Unni and Sujith.[37] During combustion noise, there is no dominant frequency, and as we approach thermoacoustic instability, there is a dominant frequency of about 120 Hz. As we approach lean blowout limit, the periodicity is lost and there is no dominant frequency in the time series signal. Further, Unni and Sujith[37] observed a slight variation in the dominant frequency as the equivalence ratio is varied, which was attributed to varying flame dynamics.

The adjacency matrix obtained from the recurrence matrix represents the topology of the network. Figure 4 represents the network topologies corresponding to various dynamical regimes in the turbulent combustor. The network topology is visualized using Gephi (https://gephi.org/) software. Figure

4(a) represents the network topology for combustion noise. Figure 4(b) represents the network topology for intermittency prior to thermoacoustic instability. Figure 4(c) represents the network topology for thermoacoustic instability. The structure of the attractor is a limit cycle for thermoacoustic instability as the time series of acoustic pressure is periodic. Figure 4(d) represents the network topology for intermittency just after thermoacoustic instability. The attractor corresponding to the intermittency before thermoacoustic instability is different from that of the intermittency just after thermoacoustic instability. This is because the periodic bursts during intermittency, occurring past thermoacoustic instability, are present for a longer duration in contrast to the periodic bursts during the intermittency prior to thermoacoustic instability. Figure 4(e) represents the network topology for the aperiodic oscillations prior to lean blowout. We can observe that the network topology resembles the geometry of the attractor. Thus, we can reaffirm that RN preserves the geometry of the attractor. Figure 4(f) represents the network topology for white noise. We observe that the attractors corresponding to the time series of acoustic pressure are significantly different from the attractor corresponding to white noise. We can also observe that the nodes in the networks corresponding to that of combustion noise [Fig. 4(a)] and low amplitude aperiodic oscillations prior to blowout [Fig. 4(e)] have a lower degree compared to the degree of the nodes in the networks corresponding to intermittency and thermoacoustic instability. The degree of the nodes

in the network corresponding to white noise is very less compared to the RNs constructed from the time series of acoustic pressure.

A. Variation of degree distribution with recurrence threshold

We say that the degree distribution follows a power law if $P(k) = k^{-\gamma}$, where γ is the power law exponent. We study the variation of $log(P(k))$ vs $log(k)$ with the recurrence thresholds, $\varepsilon = 0.2$, 0.25, 0.3, and 0.35 for the RNs constructed from the time series data of acoustic pressure for various dynamical states.

Figures 5 and 6 depict the variation of degree distribution of RN constructed from time series acquired during combustion noise ($\phi = 0.98$) and aperiodic oscillations prior to lean blowout ($\phi = 0.29$). We can observe that the degree distribution follows a power law for the thresholds 0.2, 0.25. As the threshold increases, a significant portion of the degree distribution does not follow a power law. Theoretically, we say that there is a power law, if the whole distribution follows a power law, i.e., there should not be any outliers. As we are considering time series from a practical system, the entire degree distribution may not follow a power law. We need to account for some outliers. In our present work, we consider a degree distribution to follow a power law if more than 90% of the points in the degree distribution follow a power law. Figures 7, 8, and 9 depict the variation of the degree distribution of RN constructed from the time series acquired during intermittency before thermoacoustic instability ($\phi = 0.8$), during thermoacoustic instability ($\phi = 0.5$), and during intermittency just after thermoacoustic instability ($\phi = 0.47$). We can see that the degree distribution does not follow a power law for any of the chosen thresholds.
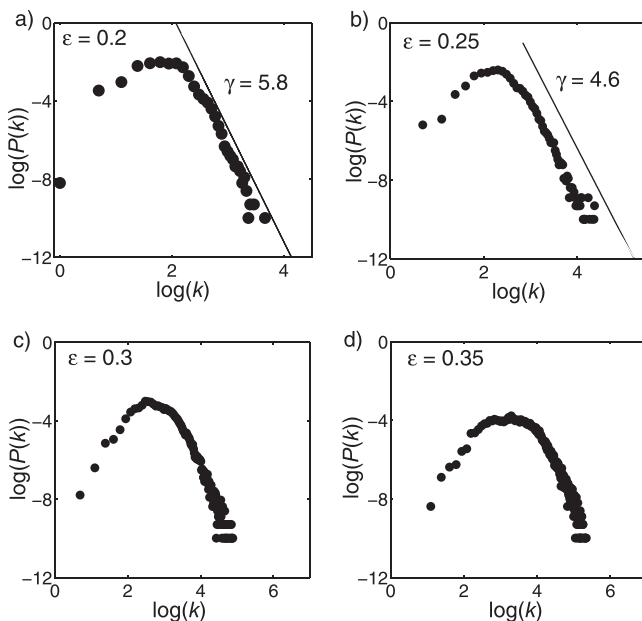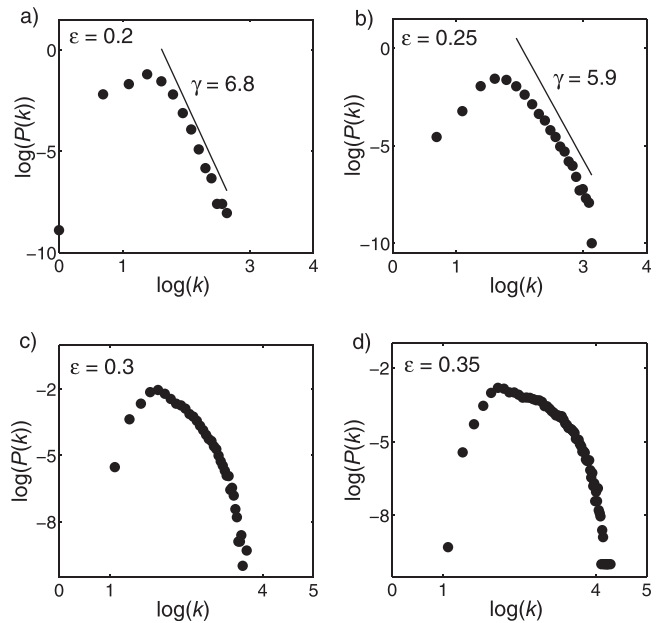

FIG. 6. The variation of $log(P(k))$ vs $log(k)$ of recurrence networks constructed from the time series corresponding to low amplitude aperiodic oscillations prior to lean blowout. ($\phi = 0.29$) with various thresholds $\varepsilon = 0.2$, 0.25, 0.3, and 0.35, respectively. The width of the degree distribution is less and the power law is significant for lower thresholds.

The long term distribution (invariant measure) of the phase space vectors of a dynamical system is associated with a probability distribution[38] of an invariant measure. The time for which a state stays at a particular location in phase space can be associated with an invariant density at that location. Thus, a probability distribution can be associated with the invariant density distribution over the attractor. The degree distribution determines the local connectivity pattern of a
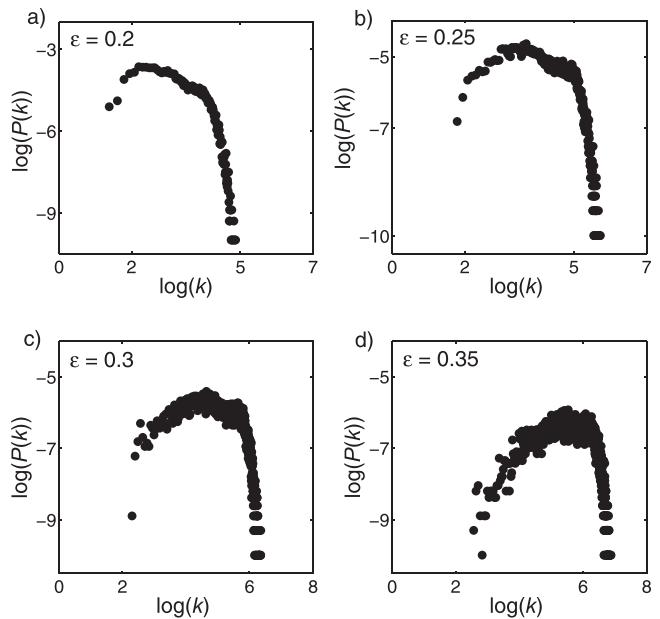

FIG. 5. The variation of $log(P(k))$ vs $log(k)$ of recurrence networks constructed from the time series corresponding to combustion noise ($\phi = 0.98$) with various thresholds $\varepsilon = 0.2$, 0.25, 0.3, and 0.35, respectively. We can see that the power law is significant at lower thresholds.

FIG. 7. The variation of $log(P(k))$ vs $log(k)$ of recurrence networks constructed from the time series corresponding to intermittency prior to thermoacoustic instability ($\phi = 0.8$) with various thresholds $\varepsilon = 0.2$, 0.25, 0.3, and 0.35, respectively. We can see that the degree distribution does not follow a power law.
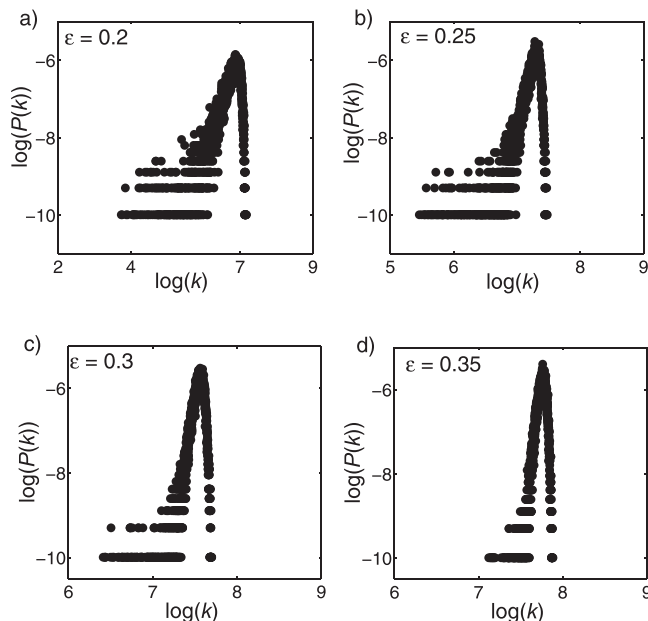
FIG. 8. The variation of $log(P(k))$ vs $log(k)$ of recurrence networks constructed from the time series corresponding to combustion instability ($\phi = 0.5$) with various thresholds $\varepsilon = 0.2$, 0.25, 0.3, and 0.35, respectively. We can see that the degree distribution does not follow a power law.

node. As the recurrence network preserves the geometry of the attractor, there is a direct mapping between the degree distribution and the invariant density over the attractor.[39] Therefore, the presence of power law in the degree distribution can be attributed to the presence of power law in the invariant density function. In a strict sense, if the invariant density function has a power law peak at some state X_0, i.e., of the form $f(X - X_0)^{-\lambda}$, for some $\lambda > 0$, then X_0 is a singularity. In a general case, if the invariant density function is close to power law at the state X_0, this results in power law
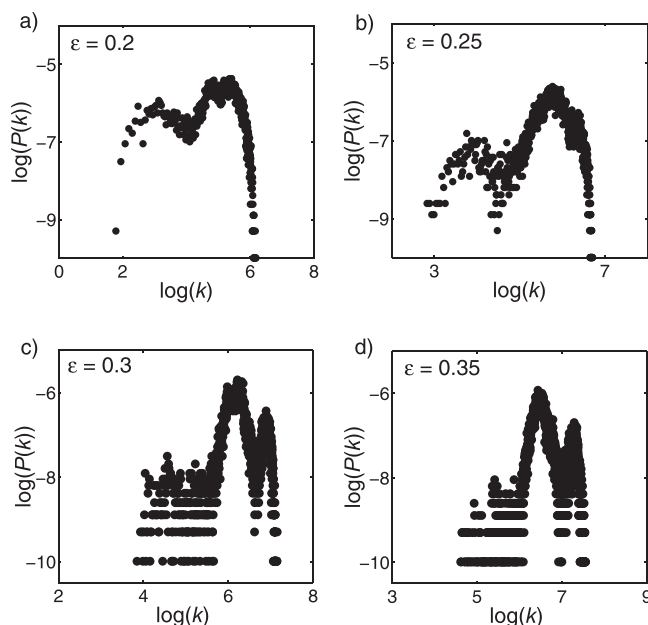

FIG. 9. The variation of $log(P(k))$ vs $log(k)$ of recurrence networks constructed from the time series corresponding to intermittency ($\phi = 0.47$) with various thresholds $\varepsilon = 0.2$, 0.25, 0.3, and 0.35, respectively. We can see that the degree distribution does not follow a power law for these thresholds.

in degree distribution. The invariant density in phase space is maximum near the singularity; hence, the phase space trajectories closer to the singularity tend to converge and the recurrence rate will be more near the singularities. The nodes closer to the singularity have a very high degree when compared to the nodes which are away from the singularity.

We observe that the presence of power laws in the degree distribution of RNs corresponding to combustion noise and the oscillations prior to lean blowout is significant only at lower thresholds such as 0.2 and 0.25. This is because the threshold corresponds to the local correlations over the reconstructed attractor in the phase space. We can state that for higher thresholds, the singularities that are local properties are masked by too many links. The invariant density changes as the recurrence threshold changes and hence the power law exponent also varies with the threshold. Further, Jacob *et al.*[39] have reported that the recurrence networks from chaotic attractors with a continuous invariant density function do not exhibit a scale free topology. As there are power law degree distributions in RNs corresponding to combustion noise and oscillations prior to lean blowout, we can state that the invariant density distribution over the attractors corresponding to combustion noise and the oscillations prior to lean blowout has singularities when lower thresholds such as 0.2 and 0.25 are used.

B. Variation of measures derived from RN with equivalence ratio

We proceeded to determine the impending transitions from combustion noise to lean blowout using measures such as characteristic path length and betweenness centrality derived from RN.

For the construction of RN from the time series of acoustic pressure, we consider $\varepsilon = 0.25$ for the calculation of topological measures of the network as the threshold ensures that there is a single component in the network without any disconnected nodes. The recurrence threshold ε also ensures that the RN constructed from the time series corresponding to combustion noise is different from the RN constructed from a stochastic process (white noise).

For most of the recurrence networks, the plot between $P(k)$ and k depends on the number of data points used for the construction of RN. The degree distribution shifts to the right with the increase in the number of data points (N) that are used to construct RN as the average degree increases with N. In order to avoid this dependence on N, the graph is plotted between the rescaled variables $P(k)N$ and k/N[30] for various equivalence ratios as shown in Fig. 10. Figures 10(a) to 10(e) correspond to the degree distributions of combustion noise, intermittency prior to thermoacoustic instability, thermoacoustic instability, intermittency just after thermoacoustic instability, and the oscillations prior to lean blowout, respectively. Figure 10(e) corresponds to the degree distribution in the network corresponding to white noise. In order to provide vivid variation of degree distributions, corresponding to combustion noise and the oscillations prior to lean blowout, zoomed in views are plotted in Figs. 10(g) and 10(h), respectively.
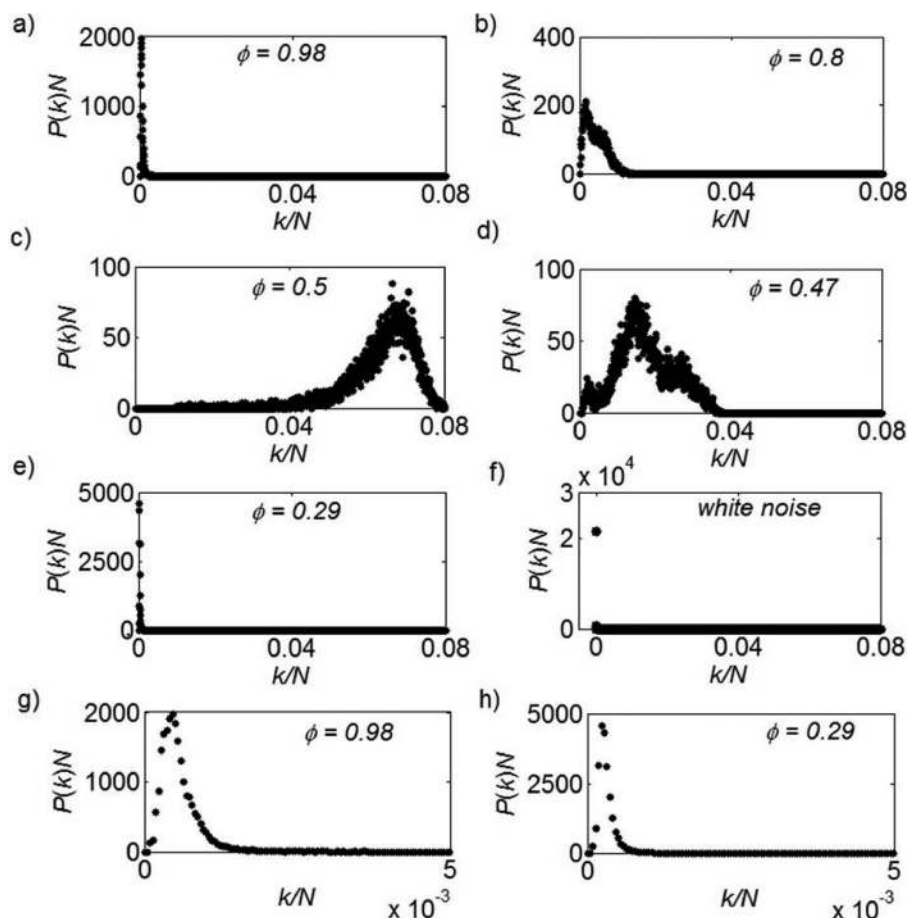
FIG. 10. The variation of degree distribution of the RNs constructed from the time series data of acoustic pressure with equivalence ratios (a) 0.98 (combustion noise); (b) 0.8 (intermittency before thermoacoustic instability); (c) 0.5 (thermoacoustic instability); (d) 0.47 (intermittency just after thermoacoustic instability); (e) 0.29 (oscillations prior to lean blowout); and (f) white noise. There is only one point (abscissa is zero) in degree distribution corresponding to white noise as there are no connections in RN when $\varepsilon = 0.25$. The zoomed in views of the degree distributions of (g) combustion noise and (h) oscillations prior to lean blowout are shown for clear visibility of the degree distribution. We used $N = 10\,000$ data points and $\varepsilon = 0.25$.

As we decrease the equivalence ratio from 0.98 to 0.5, the degree distribution shifts to the right. The degree distribution of RN corresponding to thermoacoustic instability [Fig. 10(c)] is concentrated at a higher degree indicating higher connections. Hence, the phase space density at those locations is high over the attractor. We can also see in Fig. 10(c) that there is a single prominent peak. Such a peak in the degree distribution concentrated at higher degree corresponds to a periodic signal.[40] This reaffirms that thermoacoustic instability is periodic. The degree distribution corresponding to $\phi = 0.47$ [Fig. 10(d)] has multiple peaks in the degree distribution and the degree distribution is broad. Similarly, the degree distribution corresponding to the equivalence ratio $\phi = 0.8$ [Fig. 10(b)] is also wide spread. This implies that there are large fluctuations in phase space density over the attractor. During the intermittent regime, there are large amplitude periodic fluctuations amidst the aperiodic oscillations, hence leading to the fluctuations in the local phase space density over the attractor.

We observe that the degree distribution shifts to the left, when we decrease the equivalence ratio from $\phi = 0.5$ to $\phi = 0.29$, and becomes more concentrated towards lower degree. This implies that the link density of RN constructed from the time series data prior to lean blowout is less. The duration of the periodic bursts in the signal decreases as the transition occurs from thermoacoustic instability to blowout. As the recurrence rate is less, the phase space density is less which results in a shift in the degree distribution towards the left as the transition happens from thermoacoustic instability

to blowout. Therefore, the recurrence rate decreases and also the average degree of the nodes decreases.

The peak in the degree distribution in the RN corresponding to the oscillations prior to lean blowout is concentrated towards lower degree than in the RN corresponding to combustion noise (Fig. 10). As the degree distribution can be mapped to the phase space density, the average density in phase space is less for the oscillations prior to lean blowout. This results in a lower degree of recurrence for the oscillations prior to blowout. We also observe that the degree of all the nodes is zero in the RN corresponding to white noise [Fig. 10(f)]. This is because there are no connections between the nodes in the RN constructed from white noise using the threshold $\varepsilon = 0.25$ (Fig. 1).

Figure 11 shows the variation of *CPL* with the equivalence ratio. *CPL* is minimum for the RN corresponding to thermoacoustic instability and maximum for the RN corresponding to the oscillations prior to blowout. *CPL* measures the spatial distance between two nodes which are nothing but two states. For a periodic signal, the recurrences in the phase space are more and hence the shortest path between two nodes is less and *CPL* is minimum for thermoacoustic instability. *CPL* is high for the oscillations prior to lean blowout and combustion noise as the average degree and the recurrence rate are less when compared with thermoacoustic instability.

Figure 12 shows the variation of the average betweenness centrality with the equivalence ratio. We observe lower values of betweenness centrality for thermoacoustic instability and very high values for combustion noise and the
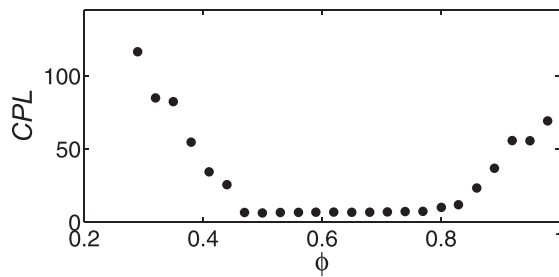
FIG. 11. Variation of *CPL* with equivalence ratio. *CPL* is high for RN corresponding to combustion noise and decreases as we approach thermoacoustic instability. *CPL* again increases as we approach lean blowout limit. *CPL* varies with the dynamical regime. Hence, *CPL* can be used to detect the transitions from combustion noise to thermoacoustic instability and the transitions from thermoacoustic instability to lean blowout. We used $N = 5000$ data points and $\varepsilon = 0.25$.

oscillations prior to lean blowout. Betweenness centrality gives the information related to the presence of regions with a low phase space density that separates the regions of a high phase space density. High values of betweenness centrality indicate that the attractor has high local fragmentation.[36] As the thermoacoustic instability is periodic, there will be uniform distribution of the regions with a high phase space density. Hence, betweenness centrality is low for thermoacoustic instability.

The network measures characteristic path length and betweenness centrality captures the transitions from combustion noise to thermoacoustic instability and from thermoacoustic instability to blowout. Hence, these measures can be used to measure the proximity to an impending transition in turbulent combustor, in industrial applications.

V. CONCLUSIONS

We introduce recurrence networks to study the transitions between the dynamical regimes in a combustor with a turbulent reactive flow, for the first time. We observed that the network topology represents the geometry of the attractor in phase space. The network topology varies with the dynamical regimes. The network topology of RN constructed from white noise is completely different when compared with the topologies of RNs constructed from the time series of
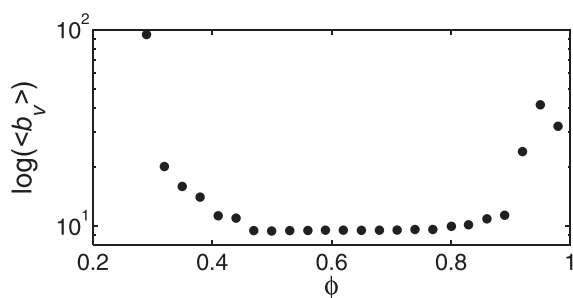

FIG. 12. Variation of logarithmic value of average betweenness centrality in log scale with equivalence ratio. $\langle b_v \rangle$ is high for the RN corresponding to combustion noise and decreases as we approach thermoacoustic instability. $\langle b_v \rangle$ again increases as we approach lean blowout limit. Betweenness centrality varies with the dynamical regime and, hence, can be used to detect the transition from combustion noise to thermoacoustic instability and the transition from thermoacoustic instability to lean blowout. We used $N = 5000$ data points and $\varepsilon = 0.25$.

acoustic pressure for various equivalence ratios. The average degree and hence the recurrence and the degree of determinism are higher for the RNs constructed from the time series of acoustic pressure when compared with the RN constructed from white noise. As the transition happens from combustion noise to thermoacoustic instability, the corresponding topology of the attractor changes from a complex topology to a limit cycle. During the transition from thermoacoustic instability to lean blowout, the topology of an attractor changes from a limit cycle to a complex topology. Thus, the topology of RN is different for different dynamical regimes. The plot of degree distribution in RN shows the presence of power law degree distribution in the recurrence networks constructed from the time series of acoustic pressure corresponding to combustion noise and oscillations prior to lean blowout. The presence of power law is due to the presence of singularities in the invariant density. We then proceeded to study the variation of the measures derived from RN with equivalence ratio. We observed that the variation of the network measures *CPL* and betweenness centrality with equivalence ratio is able to detect the transitions in a turbulent combustor and hence can be used as early warning signals. We henceforth conclude that RN can be used as a potential tool to capture the transitions between the dynamical regimes in a turbulent combustor, in industrial applications.

[1]R. I. Sujith, M. P. Juniper, and P. J. Schmid, Int. J. Spray Combust. Dyn. **8**, 119 (2016).
[2]L. Kabiraj, R. I. Sujith, and P. Wahi, J. Eng. Gas Turbine Power **134**, 031502 (2012).
[3]J. Tony, E. A. Gopalakrishnan, E. Sreelekha, and R. I. Sujith, Phys. Rev. E **92**, 062902 (2015).
[4]V. Nair, G. Thampi, S. Karuppusamy, S. Gopalan, and R. I. Sujith, Int. J. Spray Combust. Dyn. **5**, 273 (2013).
[5]V. Nair and R. I. Sujith, J. Fluid Mech. **747**, 635 (2014).
[6]V. Nair, G. Thampi, and R. I. Sujith, J. Fluid Mech. **756**, 470 (2014).
[7]L. Kabiraj, P. Wahi, and R. I. Sujith, Fluid Dyn. Res. **44**, 031408 (2012).
[8]L. Kabiraj and R. I. Sujith, J. Fluid Mech. **713**, 376 (2012).
[9]H. Gotoda, M. Amano, T. Miyano, T. Ikawa, K. Maki, and S. Tachibana, Chaos **22**, 043128 (2012).
[10]H. N. Gotoda, Y. Shinoda, M. Kobayashi, Y. Okuno, and S. Tachibana, Phys. Rev. E **89**, 022910 (2014).
[11]V. R. Unni and R. I. Sujith, in *International Congress on Sound and Vibration, July 12–16, Florence, Italy* (2015), p. 22.
[12]S. B. Johnson, *Emergence: The Connected Lives of Ants, Brains, Cities, and Software* (Scribner, 2011).
[13]M. Mitchell, Artif. Intell. **170**, 1194 (2006).
[14]A. L. Barabasi, Nat. Phys. **8**, 14 (2011).
[15]Z. Gao and N. Jin, Phys. Rev. E **79**, 066303 (2009).
[16]Z. K. Gao, N. D. Jin, W. X. Wang, and Y. C. Lai, Phys. Rev. E **82**, 016210 (2010).

[17]A. Charakopoulos, T. E. Karakasidis, P. N. Papanicolaou, and A. Liakopoulos, Chaos **24**, 024408 (2014).

[18]A. Lesne and M. Laguës, *Scale Invariance: From Phase Transitions to Turbulence* (Springer, Heidelberg, Germany, 2011).

[19]X. Xu, J. Zhang, and M. Small, Proc. Natl. Acad. Sci. U.S.A. **105**, 19601 (2008).

[20]L. Lacasa, B. Luque, F. Ballesteros, J. Luque, and J. C. Nuno, Proc. Natl. Acad. Sci. U.S.A. **105**, 4972 (2008).

[21]J. Zhang and M. Small, Phys. Rev. Lett **96**, 238701 (2006).

[22]R. V. Donner, Int. J. Bifurcation Chaos **21**, 1019 (2011).

[23]F. Strozzi, J. M. Zaldívar, K. Poljansek, F. Bono, and E. Gutiérrez, JRC Scientific and Technical Reports, EUR 23947 JRC52892 (2009).

[24]M. Murugesan and R. I. Sujith, J. Networks Complex Syst. **4**, 17 (2014).

[25]M. Murugesan and R. I. Sujith, J. Fluid Mech. **772**, 225 (2015).

[26]M. Murugesan and R. I. Sujith, J. Propul. Power **32**, 707 (2016).

[27]N. Marwan, J. F. Donges, Y. Zou, R. V. Donner, and J. Kurths, Phys. Lett. A **373**, 4246 (2009).

[28]D. Vjushina, R. B. Govindan, R. A. Monettia, S. Havlina, and A. Bundeb, Physica A. **302**, 234 (2001).

[29]J. F. Donges, R. V. Donner, M. H. Trauth, N. Marwan, H. J. Schellnhuber, and J. Kurths, Proc. Natl. Acad. Sci. U.S.A. **108**, 20422 (2011).

[30]R. Jacob, K. P. Harikrishnan, R. Misra, and G. Ambika, Phys. Rev. E **93**, 012202 (2016).

[31]F. Takens, *Lecture Notes in Mathematics* (Springer, Heidelberg, Germany, 1981), Vol. 898.

[32]L. Cao, Physica D **110**, 43 (1997).

[33]J. P. Eckmann, S. O. Kamphorst, and D. Ruelle, Europhys. Lett **4**, 973 (1987).

[34]N. Marwan, M. C. Romano, M. Thiel, and J. Kurths, Phys. Rep. **438**, 237–329 (2007).

[35]N. Marwan and J. Kurths, Chaos **25**, 097609 (2015).

[36]R. V. Donner, Y. Zou, J. F. Donges, N. Marwan, and J. Kurths, New J. Phys. **12**, 033025 (2010).

[37]V. R. Unni and R. I. Sujith, J. Fluid Mech. **784**, 30 (2015).

[38]G. Froyland, O. Junge, and P. Koltai, SIAM J. Numer. Anal **51**, 223 (2013).

[39]R. Jacob, K. P. Harikrishnan, R. Misra, and G. Ambika, Phys. Lett. A **380**, 2718 (2016).

[40]R. Xiang, J. Zhang, and M. Small, in *International Symposium on Nonlinear Theory and its Applications* (2010), p. 589.